



Geometrical parameters and strength of clinching joint formed with the use of an additional rivet

Jacek Mucha¹ · Łukasz Boda² · Waldemar Witkowski¹

Received: 20 January 2023 / Revised: 15 March 2023 / Accepted: 26 March 2023
© The Author(s) 2023

Abstract

In the publication, the results of an experimental analysis of joint formation by pressing of DX51D steel sheets with thickness of 1.5 (mm) with the use of a rigid punch and an additional deformable rivet of various shapes were presented. The influence of the use of a steel rivet with a diameter $d = 5$ (mm), similar to the dimensions of the forming punch in the case of the classic clinching variety on the interlock parameters was investigated. The used die was with a four movable segments—dedicated to connections made in the clinch-riveting technology by TOX[®] PRESSOTECHNIK. In additional, experimental tests were made for joining sheets with a rivet of various shapes, i.e. with a through hole. Joints were formed and the correctness of the upper blockage in the lower sheet was observed on the joints cross-sections. The interlock parameters were measured for each joints samples. In order to compare the influence of using an additional rivet on interlock parameters and joints strength the traditional clinching joints were also made. The minimal thickness of the traditional clinching joint embossment for 2 sheets of 1.5 (mm) thickness for each was $X = 0.75$ (mm).

Keywords Clinching joints · Clinch-riveting · Rivet hole · Clinching joints strength · Forming force

1 Introduction

The use of the thin-walled structures in many industries is still increasing. The energy saving, products weight reducing and environmental protection issues are very important to manufacturers and consumers. Ou et al. [1] presented optimization technologies for body-in-white development project. In three steps of optimization (frame material distribution, joints distributions and all parts topology), they reduced the weight of car frame (innovative design was 13.3% lighter than the base design). New joining technologies and also traditional joining techniques are still improved. The

thin-walled structures can be joined not only by traditional joining process like resistance spot welding, riveting, festering, etc. but also by joint plastic forming process [2]. Most popular pressed joints are clinching joints [3]. Recent developments in clinching process like rectangular clinching, dieless clinching, flat clinching, hole clinching, roller clinching, laser shock clinching, hydro-clinching, injection clinching, adhesive clinching, resistance spot clinching, friction-assisted clinching, laser-assisted clinching and reshaping the clinched joint with/without a rivet were introduced by Peng et al. [4]. Novel methods of tool design and joining optimization of clinching process and suggested future trends are described by Zhang et al. [5]. Zhang et al. [6] presented modification of clinching punch for joining aluminum alloy. By using modified punch geometry, they obtained the increase of joint tensile and shear strengths. To reduce experimental tests of new or modified tolls and joining technology modifications, researchers are widely using FEM simulation. Based on 2D and 3D models, they obtaining not only interlock parameters but also joint tensile and shear strength, joint failure mechanism, tools position accuracy and others [7].

Clinch-rivet joining is a development of clinching joining technology. The ClinchRivet[®] technology was patented by TOX[®] Pressotechnik. The rivet used in these connections is

✉ Jacek Mucha
j_mucha@prz.edu.pl

Łukasz Boda
d413@stud.prz.edu.pl

Waldemar Witkowski
wwitkowski@prz.edu.pl

¹ Faculty of Mechanical Engineering and Aeronautics, Rzeszow University of Technology, al. Powstancow Warszawy 8, 35-959 Rzeszow, Poland

² Doctoral School of the Rzeszów University of Technology, al. Powstancow Warszawy 12, 35-959 Rzeszow, Poland

a cylindrical rivet. The main advantages of clinch-riveting joining are: the use of additional rivet with symmetrical geometry and no sheet material cutting from any side (punch or die side). The surface coating, due to no sheet cutting, is also without damage, so the joints are more resistant to corrosion than in self-piercing riveting. Joint forming tools are more complex than in case clinching tools—special mechanism to applying additional rivet in the joint and extensible die are necessary [8].

The strength of clinch-rivet joints in compare with clinching joints, self-piercing riveting joints, blind rivet joint, self-drilling screw joints is presented in some papers. For S350GD steel sheets, the analysis of strength and failure mechanism for single and double arrangement of joints were presented by Mucha et al. [9]. The strain direction change by 90°, for double joint arrangement, caused 50% increase of the maximum shearing force. For different loading force angle, the clinch-rivet joints strength and failure mechanism were presented by Mucha et al. [10]. In comparison with clinching joints the clinch-rivet joints loading force was higher about 50% for each load force angle.

The failure mechanism for clinch-rivet joints is different than for clinching. In the tensile shearing test, the additional rivet, locked in the sheets, prevents complete shearing. The sheet separation occurs by pulling out the upper sheet from bottom sheet. In clinching joint shear tests, the fracture mode are neck fracture and button separation [10].

An additional rivet applied in clinching joint, in separate process, can be used to repair deformed/damaged clinching joints. Pressing rivet in clinching joint generates new interlock parameters—can reshape deformed/damaged interlock. Chen et al. [11] proposed to use an additional solid rivet, in separated process, to increase the joint strength and to decrease the embossment (protrusion) height. The upsetting force in second step of joining process (rivet pressing in clinching joint) influenced on the protrusion height and cross-tension strength. In [12] Chen et al. presented the FEM simulation of clinched joint reshaping process. They analyzed the strain and stress distribution in reshaping process with and without an additional rivet. Optimization of the shape of an additional rivet, used in reshaping process of clinching joints, was presented by Chen et al. [13]. In paper [14], Chen et al. discussed the influence of the joints damaging force on the joints strength (after reshaping by pressing an additional rivet). Chen et al. [15] compared the clinched joints with renovated deformed clinched joints and with renovated damaged clinched joints. In both case of renovation of clinched joints interlock parameters changes and influenced on increasing of joints shear strength. Shi et al. [16] presented the parameters of new interlock (after renovating of clinched joints). Obtained by increasing the repairing force. Hence, the repaired clinch joints tensile and shear strength also increased.

The use of an additional rivet, with through hole, in separated process after clinching process was presented by Ren et al. [17]. For the rivet 1.0 mm wall thickness, the interlock value, the joint tensile strength and dissipated energy were highest, compared to joint with: no rivet, full rivet, rivet of 1.5 mm and 2.0 mm wall thickness.

New modification of clinch-rivet joining technology is flat bottom riveting presented by Chen et al. [18]. The main advantages of that new modification is flat lower surface (without protrusion) like in flat clinching. They verified FEM simulations results of interlock parameters and joints tensile strength by experimental tests. Shi et al. [16] presented flat clinch-rivet joints strength in tensile and shear tests. The failure mode observed in tests were pull-out in tensile test and shear failure with pull-out failure in shear tests.

Zhang et al. [19] proposed to combine clinch-rivet process with resistance spot welding process to join AA 5754 with DQSK steel. The energy absorption in tensile shear tests for that joints was three times higher than for spot-welded joint.

Rivet as an additional element in ClinchRivet joint is usually pressed by the punch from top sheet side. Sampaio et al. [20] presented new geometry of self-clinching fasteners (rotationally and longitudinally symmetrical), which are hidden inside between joined sheets. This joints are lighter than steel bolted joints. The electrical resistance is also smaller. After forming the joint, there is no possibility to check the continuity of fastener geometry without destroying the joint. Only crack on outside surfaces of sheets can be observed.

He et al. [21] used two rotated heads and fixed die with flat bottom to formed clinching joints for 1.5-thick A11060 sheets. Because of obtaining non symmetrical interlock the joints strength was depending on load force direction (maximum shear strength was 40% of A11060 strength, and maximum pull-out strength was 23%). For traditional clinching tools (axis-symmetrical), the shear strength is usually not depending on load force direction. The joint failure mechanism were the same like for clinching joints: pull out and pull out with neck fracture in pull-out test, neck fracture, pull out with neck fracture and pull out in the shear test.

There are not many studies on the mechanical clinching process with an additional rivet pressed in clinching joints in one process. The papers in reference are basically focused on the clinch-rivet joints with a solid rivet and its tensile shear strength. In this work, the influence of an additional rivet with through hole on the joints interlock parameters, joints strength and dissipated energy was presented. The use of an additional rivet with through hole proposed in this work contributes to decreasing the forming force and forming process energy consumption with increasing the joints strength compared to clinching joint formed with extensible die.

Table 1 Mechanical properties of sheets

| Material designation | Surface finish + Z | Young's modulus E , (GPa) | Poisson's ratio ν | Yield strength $R_{p0.2}$ (MPa) | Tensile strength R_m , (MPa) | Elongation after fracture A_{80} , (%) | Strength coefficient K , (MPa) | Strain hardening exponent n , (-) |
|----------------------|---|-----------------------------|-----------------------|---------------------------------|--------------------------------|--|----------------------------------|-------------------------------------|
| DX51D | Zinc layer quality 275 (g/m^2) | 188 | 0.3 | 330 | 438 | 29 | 593 | 0.2 |

2 Materials and methods

2.1 Experimental materials

The formed joints were used to connect two steel sheets DX51D + Z/275 (according to PN-EN 10346: 2015-09 [22], material number 1.0917) of thickness 1.5 mm. Strength properties are shown in Table 1 and chemical composition are presented in Table 2.

Tox Pressotechnik rivets with A5 \times 5-2Al catalog number were used in clinching joining process as an additional deformable element (Fig. 1a). The average hardness of the steel rivets for the five measurements was 400 HV1. The hardness was measured in accordance with the PN-EN ISO 6507-1:2018-05 standard [23]. The microstructure of the rivet material is presented in Fig. 1c.

2.2 Experimental procedure

2.2.1 Forming tools, joint arrangements and additional rivet geometry

To analysis the influence of the additional deformed element on the forming process and the strength of the pressed joint, connections were made using combination of tool presented in Fig. 2. In experimental joining of two steel sheets, with total thicknesses of 3 mm, the round clinching punch and SKB die were used. Two combinations of forming tools were used:

1. Punch ("CL") along with die contain fixed and moving segments dedicated to ClinchRivet ("CR"). This method is described as "CL/CR"—Fig. 2a.
2. Rivet ("CR") along with die contain fixed and moving segments dedicated to ClinchRivet ("CR"). This method is described as "CR/CR"—Fig. 2b.

In each of the methods mentioned above, it is important to maintain material continuity of every combined layer.

TOX Pressotechnik frame construction press type CMB, with maximum force load 100 kN and electric drive EMPK, were used to prepare joints. Punch system tools was mounted to the vertically moved drive, and the die mounted as non-movable to the bottom part of the C-frame press. The arrangements of joints were made at the Department of Machine Design at Rzeszow University of Technology.

For "CL/CR" joining method, the minimum thickness of the embossment X used for 2 sheets is 0.75 mm ($X = 25\%$ of total sheets thicknesses). This is the final position of punch measured as the distance to the bottom of the die (Fig. 3—left side). For joints with rivet ("CR/CR"), the pressing movement was realized until the upper rivet surface was leveled with the surface of the upper sheet (Fig. 3—right side). The punch positioning accuracy was 0.01 mm, and the maximum error of the measured forming force was 0.5% of the force.

Basis dimension of forming tools are shown in Fig. 4. The diameter of clinching punch (Fig. 4a) was chosen as similar to diameter of the additional rivet (Fig. 5). The "SKB" die used in experiment had a 4 movable segments, which caused that the sheet material flow in the space between fixed elements (Fig. 4b). The punch system in ClinchRivet technology is also more advanced, because it has got a rivet feeding system. A cross-section of "CL" punch holder is presented in Fig. 4c, and the "CR" rivet feeder is presented in Fig. 4d.

To investigate the influence of an additional deformable rivet shape on the forming process and strength of the pressed joint, the shape modification was prepared. Basis geometry was modified by additional through hole in rivet axis. Four diameter holes were tested $\phi d = 1.0, 1.5, 2.0, 2.5$ mm (Fig. 5b). The sheet metal specimens were cut from the steel sheets DX51D + Z/275 of thickness 1.5 mm. For each arrangement, five samples were prepared—to determine the

Table 2 Chemical composition of DX51D + Z/275 sheet (maximum content in %)

| Mn | Si | C | P | S | Ti | Fe |
|-----|-----|------|-----|-------|-----|-----------|
| 0.6 | 0.5 | 0.12 | 0.1 | 0.045 | 0.3 | Remainder |

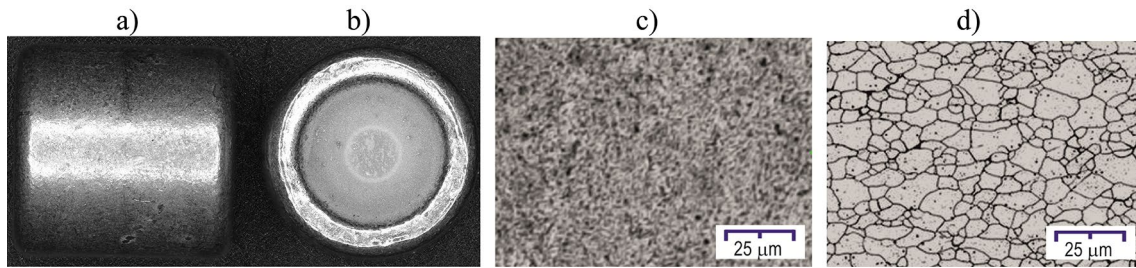


Fig. 1 Basis rivet with hardness 400 HVI real view of rivets (a), top view of used rivet (b), microstructure of used rivet (c), microstructure of DX51D steel sheet (d)

Fig. 2 Tool configuration used for forming joints: a “CL/CR”, b “CR/CR”. 1—clinching punch, 2—clinching punch side holder, 3—top sheet, 4—bottom sheet, 5—movable segments of “SKB” die, 6—“SKB” die, 7—additional rivet

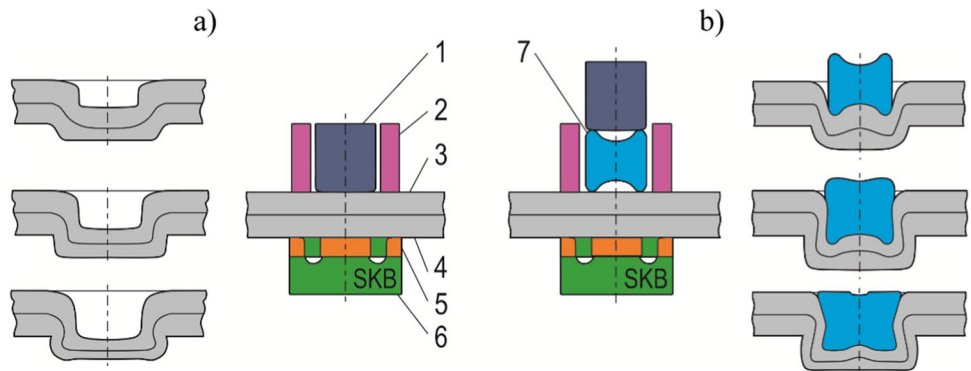
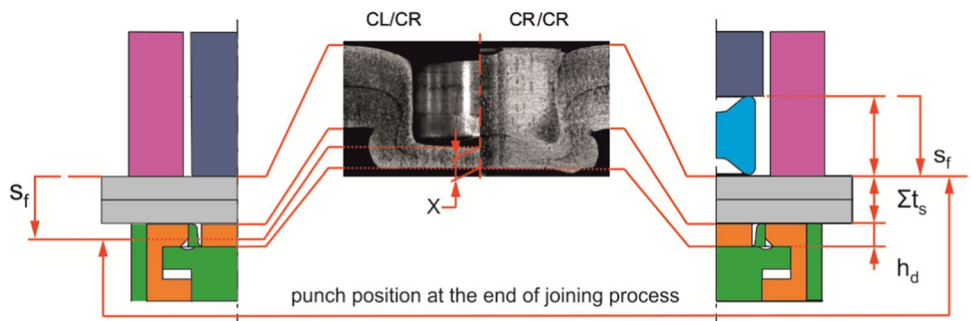


Fig. 3 The final position of forming tools for “CL/CR” method (left side), “CR/CR” method (right side). S_f —punch displacement, X —minimal thickness of the embossment, $\sum t_s$ —total sheets thicknesses, h_d —depth of the “SKB” die



average joint forming force and the average tensile shear force. The list of joints combination is presented in Table 3.

Measurements of specific geometrical features dimensions, on its cross-section, were used to analyze the quality of the joints. In order to minimize the interference in the structure of the inner line of the sheets and the rivet, the WEDM (Wire Electrical Discharge Machining) technology (AgieCharmilles Cut 30 P) was used for cutting. In addition, the selected technology ensures high cutting precision, for which the maximum dimensional error between the largest and smallest deviation from the nominal is $\pm 5 \mu\text{m}$. The surface roughness after the cutting process, in the Ra scale, is $3 \mu\text{m}$. The cut was made with a wire with a diameter of 0.25 mm .

The observation and measurements of the joints parameters (Fig. 6) were carried out using a Keyence VHX7000 optical microscope (Fig. 7). The microscope was equipped with a VH-Z20R/Z20T zoom lens of standard

Table 3 Tools arrangements and additional rivet geometry (diameter d in mm)

| Tools configurations | Additional element |
|----------------------|---------------------------|
| CL\CR | None |
| CR\CR | Basis rivet (solid rivet) |
| CR\CR | Through hole— $d = 1.00$ |
| CR\CR | Through hole— $d = 1.50$ |
| CR\CR | Through hole— $d = 2.00$ |
| CR\CR | Through hole— $d = 2.50$ |

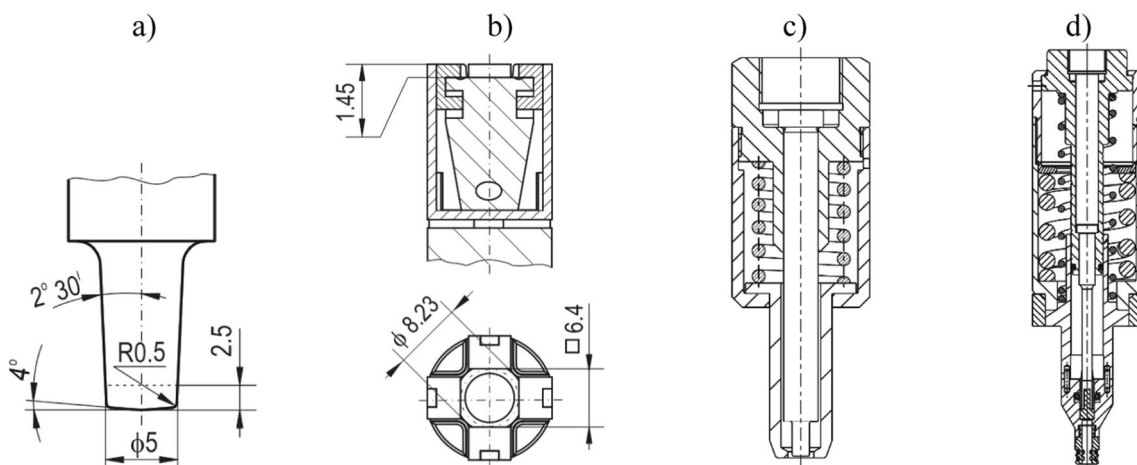


Fig. 4 Shape and geometry of tools used in joint forming processes (“CL/CR”, “CR/CR”): **a** punch, **b** “SKB” die (in mm), **c** “CL” punch system with blank holder, **d** “CR” rivet feeder with blank holder

magnifications, with which it was possible to observe with a zoom of 100x, which allowed to obtain a single image with a resolution of 2048 × 1536 px with a working area of 3.05 by 2.28 mm. The lens distance was 25.5 mm. The distance between the pixels of the recorded image was within 0.0015 mm, in both directions of the cross-section plane.

Using the fast image fusion function, the images representing the cross-section of the joints, with a resolution of 6407 × 4956 px, were obtained. The integrated VHX-7000_970F software, was used to measuring the characteristic features and dimensions of the joints geometry.

2.2.2 Joint tensile strength tests

For the static shearing tests, the sample geometry, including the size of the overlap, was determined on the basis of the guidelines contained in ISO 12996: 2013 standard [24]. The dimensions of single-lap joints for tensile shear tests are presented in Fig. 8.

For single-lap joint specimens (Fig. 8), the tensile shear tests were performed in accordance with the guidelines from

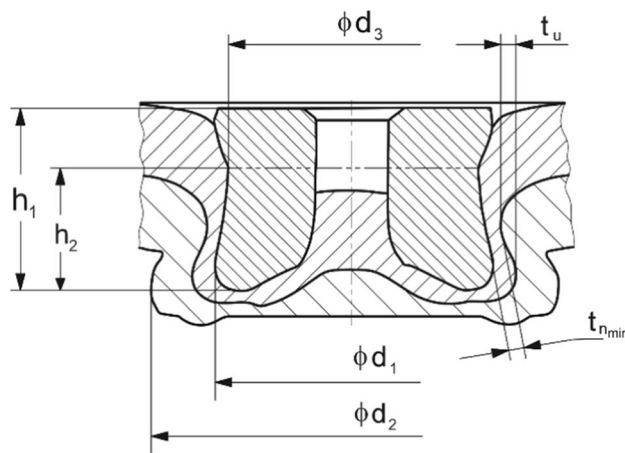


Fig. 6 The characteristic dimensions of the joint geometry (in mm)

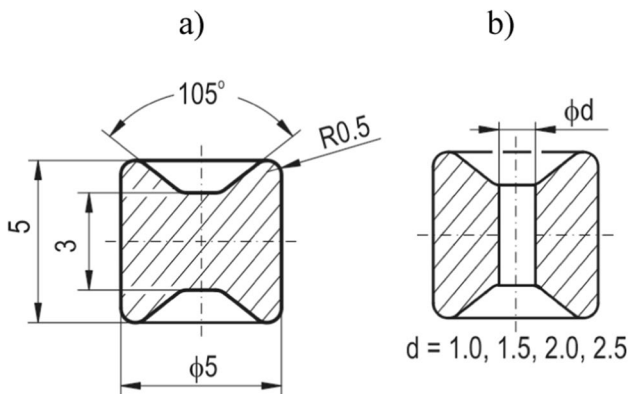


Fig. 5 Additional rivets used in “CR/CR” method: **a** standard solid rivet, **b** hollow rivet (in mm)



Fig. 7 The measurements stand

Fig. 8 Dimensions of single-lap tensile shear test specimens (in mm)

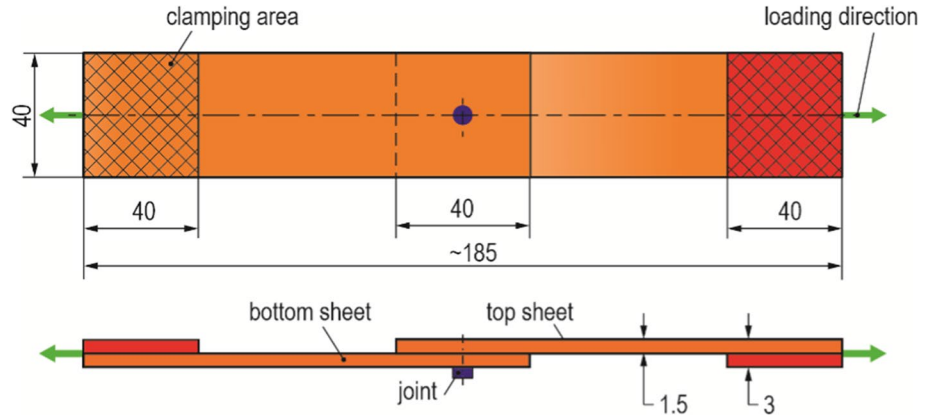
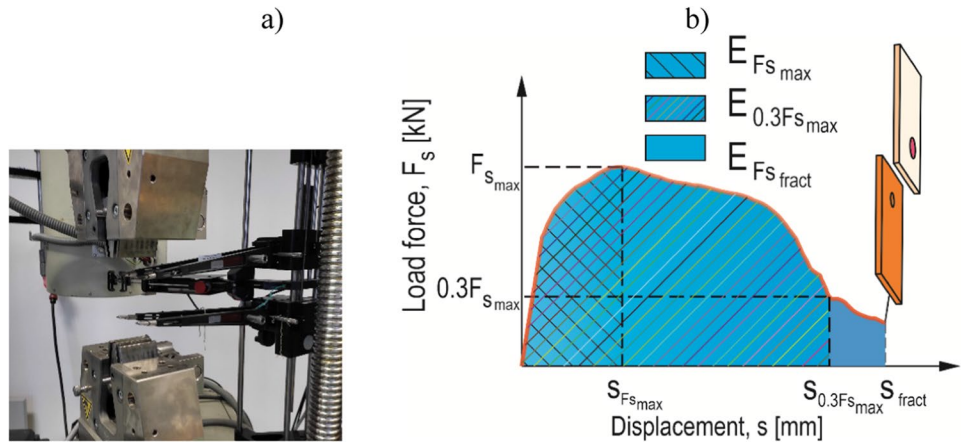


Fig. 9 Tensile shear test and dissipated energy diagram: **a** the extensometer’s measuring system used in tensile shear tests, **b** load-elongation diagram for the tensile shear test



ISO 12996: 2013. The static shear tests were performed using Instron 3382 machine. The traverse speed of the testing machine was set up to 1.6×10^{-7} m/s. The extensometer’s measuring system presented in Fig. 9a was used to measure the values of displacement. The measuring arm’s space was 50 mm. According to the ISO 12996: 2013 standard, the selected parameters (Eqs. 1–3) from the joint strength tests load-elongation diagram were determined (Fig. 9b).

$$E_{F_{S_{fract}}} = \int_{s=0}^{S_{fract}} F \cdot ds, \tag{1}$$

$$E_{F_{S_{max}}} = \int_{s=0}^{S_{F_{S_{max}}}} F \cdot ds, \tag{2}$$

$$E_{0.3F_{S_{max}}} = \int_{s=0}^{S_{0.3F_{S_{max}}}} F \cdot ds. \tag{3}$$

Description of Eqs. 1–3 are shown in Table 4.

3 Results and discussion

3.1 Joint forming process

In the case of using the “SKB” die, dedicated to forming ClinchRivet joints, it is possible to successfully joint two sheets, without the use of an additional deformable element—a rivet. The developed and widely used classical method of the sheets joining by pressing with round rigid tools allows for obtaining an axial-symmetrical joint. When forming a joint with using a die with movable segments (“SKB” die), the bottom sheet material is blocked by the top surface of the die fixed segments (similarly to the “CL” method). As the punch moves forward, the sheet material is pressed into the rectangular die cavity. When the sheet material is between the cylindrical part of the punch and the vertical walls of the die cavity, part of the material is pressed between the punch face and the die bottom. For sliding segments, the sheets material

Table 4 Equations' description for joint dissipated energy

| Symbol | Unit | Description |
|-------------------|------|---|
| $E_{F_{sfract}}$ | J | Dissipated energy up to fracture |
| $E_{F_{Smax}}$ | J | Dissipated energy up to F_{max} |
| $E_{0.3F_{Smax}}$ | J | Dissipated energy up to $0.3F_{max}$ |
| F | N | Tensile shear load |
| s | m | Displacement |
| s_{fract} | m | Displacement up to fracture |
| $s_{F_{Smax}}$ | m | Displacement at the maximum load F_{Smax} |
| $s_{0.3F_{Smax}}$ | m | Displacement at $0.3F_{Smax}$ |

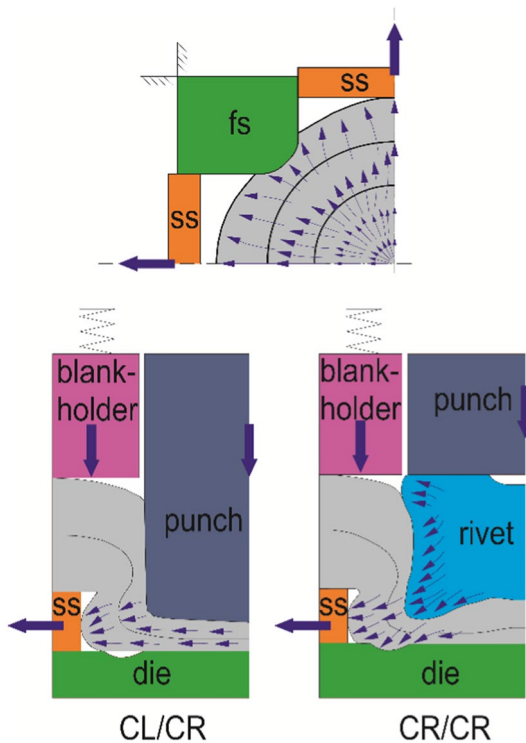


Fig. 10 The sheet material flow directions in the last phase of joining process for the “CL/CR” and “CR/CR” joints (ss—sliding segments, fs—fixed segments)

flows radially—a local interlock of the sheets is gradually formed—Fig. 10.

Instead of “CR/CR” joints, the space formed by the punch in the case of the “CL/CR” tool combination (Table 3) is filled by a deformable additional rivet (Fig. 11). In the photos presented in Fig. 11, it can be seen that in the case of forming the “CL/CR” joint, the sheets pressure on the top surface of the sliding segments results in a different impress (line 1). The use of an additional rivet increased the sheet material flow in the radial direction, so that the impression line (line 1—Fig. 11—“CR/CR” joint) was obtained with the edges of the sliding segments. In the paper, the impact of

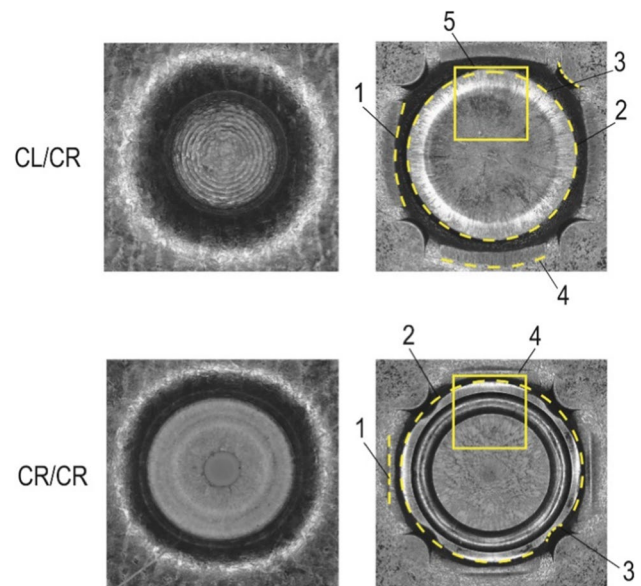


Fig. 11 View of the joints formed by punch and SKB die (“CL/CR”), and punch, “SKB” die and additional solid rivet (“CR/CR”) (on left view from punch side, on right view from die side)

the use of an additional rivet on the size of the joint outer diameter (determined by a circle—line 2) was presented. The flow rate of the sheet metal material during the formation of the “CR/CR” joint is so high that sheet material was strongly pressed to the fixed segments of the die (line 3).

For the joint forming with the use of the punch (“CL”) and the “SKB” die, in the last phase of pressing, the material flow intensively in the radial direction (perpendicular to the direction of the punch movement). In order to reduce the flow resistance of the sheet material, especially the upper sheet, the punch had a front surface with a specific angle (Fig. 4a). As the punch was pressed into the sheets, they are intensively tensioned in the direction of the punch movement. This tensioning occurs for a long time without contact of the bottom sheet with the surface of the die bottom. After sheet contact with the die bottom the sheet material is strongly pressed (Fig. 2). This is why the forming force increase more intensively (Fig. 12). At this stage, the thickness of the sheets in the bottom of the embossment decreases. The intensive flow of the sheet material resulted in the fact that no ring-shaped bulge of the material appeared on the outer surface of the embossment (Fig. 11). In Fig. 12, the total force–displacement curves of “CL/CR” and “CR/CR” joining technologies were shown. For “CL/CR” technology, the punch holder (spring element) force was taken in to account—Fig. 4c. For “CR/CR” technology, the punch holder (spring element) force and rivet feeder force were taken in to account—Fig. 4d. The total forming forces in the joining processes and the corresponding energy

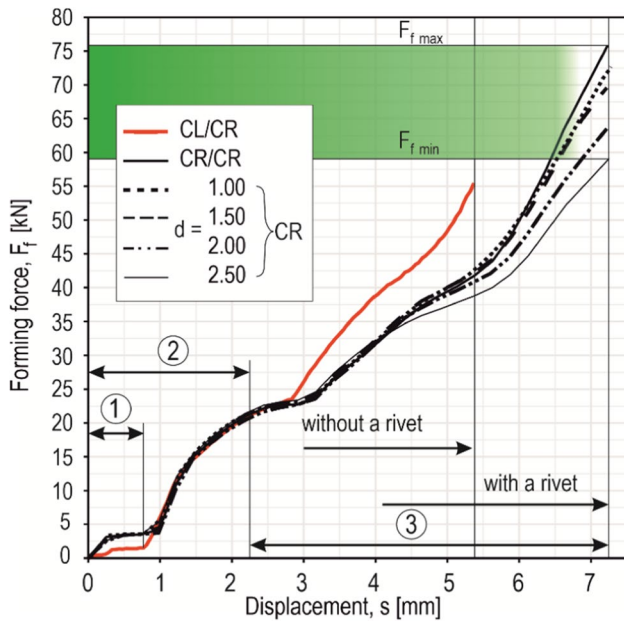


Fig. 12 Forming force diagrams for joint formed with the use of the “SKB” die (1—displacement of blank holder “CL/CR”, 2—displacement of spring deformation and displacement of rivet feeding “CR/CR”, 3—displacement of rivet pressing)

consumption of the joining process were compared in further part of paper.

The use of a deformable element (rivet) for forming joints caused that the part of the sheet material, in the axis of the rivet, was blocked. The rounded flange of the rivet intensively pressed the material towards the die groove (Fig. 10). In the last phase of joining, the rivet pressed the sheet material in the direction of possible material flow (in the radial direction). The rivet material near its axis was blocked to flow as much as the material from the area near the die segments. A dead zone was obtained in the axis of the rivet (a zone of material movement in the direction of punch travel). The cone-shaped recesses made in the rivet (Fig. 5a) caused the reduce of the area in which the sheet material flow is in the direction of the punch movement. Due to the non-uniform pressure between the sheet and the die surface, the areas of sheet more intensive tensing were formed (Fig. 13a). Micro-areas of slippage of the bottom sheet material on the outer surface of the embossment were formed (Fig. 13b).

The use of an additional rivet with 1 mm diameter through hole resulted in 5% decrease in forming force compared to the solid rivet (Fig. 12). In the case of pressing a rivet with a through hole with a diameter of 1.5 mm, the reduction of the forming force was 10.5% of the value as for a solid rivet. The enlargement of the through hole diameter to 2.0 mm reduced the maximum forming force by 17%, in relation to the formation of a joint with a solid rivet. The use of a rivet with a through hole of 2.5 mm diameter resulted

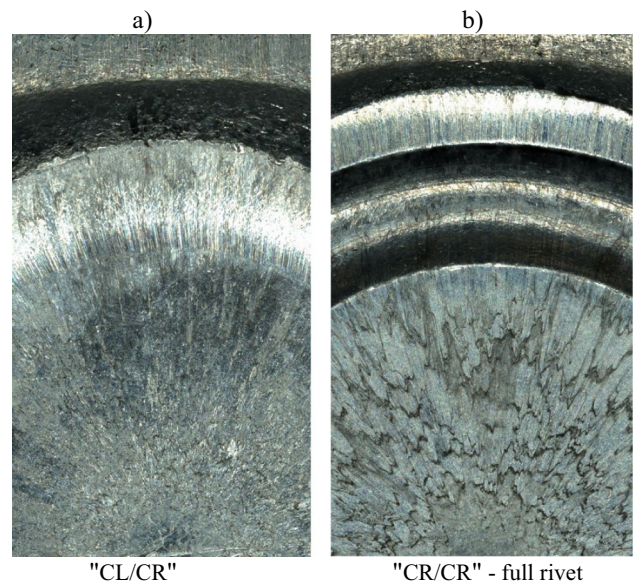


Fig. 13 The zoom of the joint embossment outside surfaces (areas number 5 from Fig. 11a and number 4 from Fig. 11b)

in a decrease in forming force by 22.5%. Observing the value of the largest dimension of the embossment from the die side (bottom sheet), it can be seen that this dimension (ϕd_2) slightly decreases as the rivet hole diameter increase (Fig. 14). The influence of the rivet hole diameter on the maximum forming force and the forming energy is shown in Fig. 15. The basic variant assumed to joint parameter calculation was the “CR/CR” joint formed with the use of a solid rivet. The highest percentage differences between the maximum forming force and the forming energy were obtained for the “CL/CR” joints and for the “CR/CR” joints in case of using a solid rivet with a hole diameter of 2.5 mm (Fig. 15).

3.2 Interlock parameters

The use of an additional rivet resulted in a greater directional displacement (radial) of the bottom sheet (Figs. 16, 17). The use of a rivet with a through hole caused that the sheet material moved in to the rivet hole (Fig. 18). In the case of “CR/CR” joints with solid rivet, in the contact area between rivet and upper sheet (in rivet axis), there is an area in which the sheet material has difficult flow conditions. Classically, during upsetting, the dead zone (the area in which there is no deformation) is observed.

The use of a rivet with a hole causes a slightly different upper sheet material flow (Figs. 10, 19). The higher diameter of rivet hole, the more upper sheet material was pressed into rivet hole (Fig. 19). Due to the rivet hole in axis, in the early phase of rivet pressing, the sheet material was not displaced in the direction of the punch movement. From rivet lower

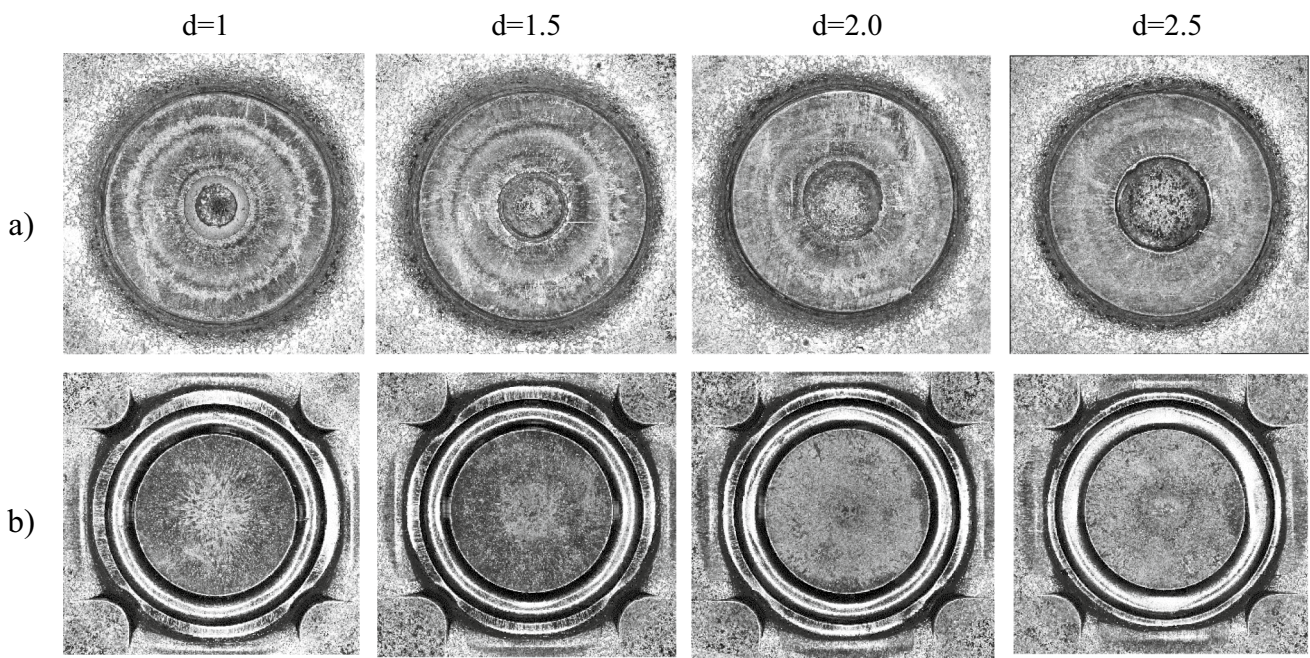


Fig. 14 Joints formed with the use of the rivet with a through hole: **a** punch side view, **b** die side view (d in mm)

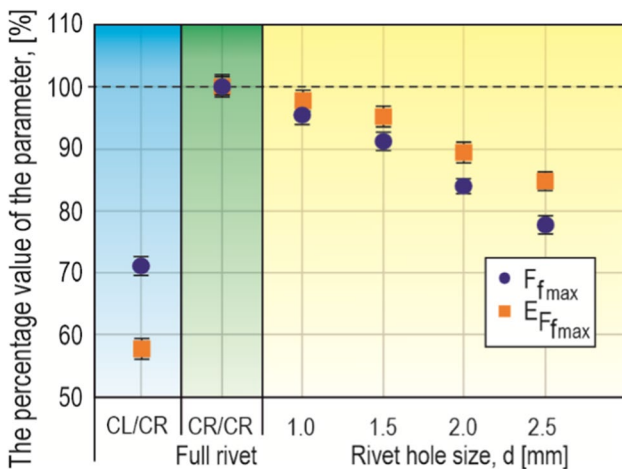


Fig. 15 Percentage value of the joint forming force (F_{fmax}) and forming energy (E_{Ffmax}) (d in mm), compared to “CR/CR” joint

surface, with rounded edge, the sheet material was pushed in transverse directions (Fig. 19). The smallest sheet thickness in the embossment was obtained for the rivet with 2.5 mm hole diameter. It should be noted that the larger rivet hole, the larger is the friction surface. The rivet hole diameter was selected so that the material coherence of the joined sheets would not be lost (this would be a process similar to self-piercing riveting).

For calculation, the solid rivet weight a several hundred of rivets were weighed. The weight of several hundred solid rivets was divided by number of rivets. For rivets with

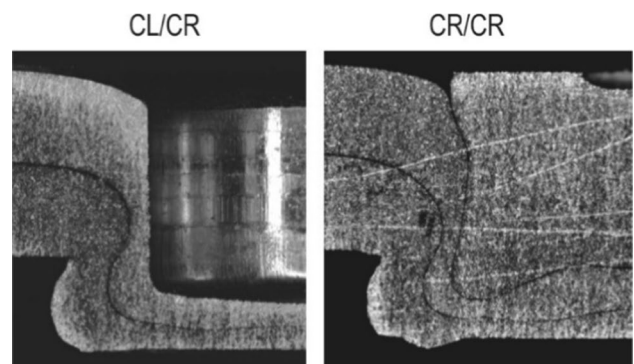


Fig. 16 Cross-section views of joints for different tool arrangement

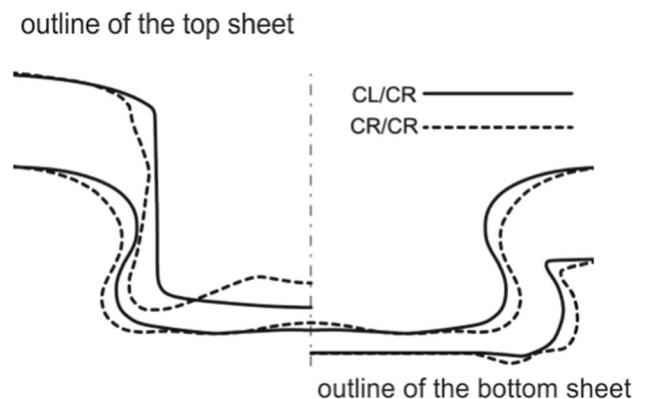
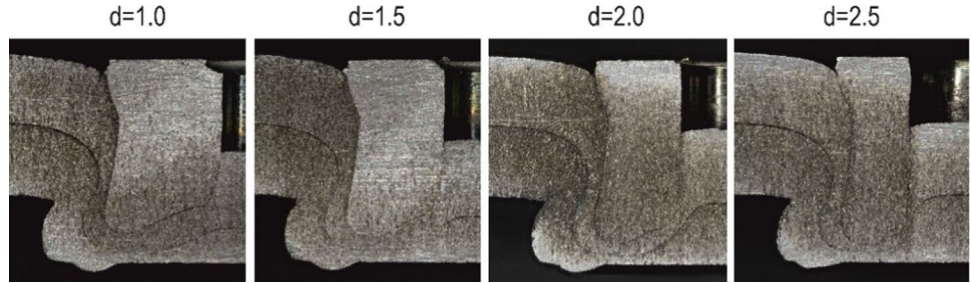


Fig. 17 Joints cross-section profiles for different tool arrangements: right side—bottom sheet, left side—upper sheet

Fig. 18 Cross-section views for joints with rivet and through hole diameters (d in mm)



through hole, the weight was calculated as weight of several rivets divided by number of rivets. Then, they were compared and presented in Table 5. The use of a 1.0 mm hole in the rivet resulted in a decrease in the weight of the rivet by 2.65%. Increasing the diameter of the rivet hole to 1.5 mm resulted in a 6.19% decrease in the weight of the rivet. And increasing the hole to 2.5 mm resulted in a 19.47% reduction in the mass of the rivet. The influence of the use of a solid rivet and a rivet with a through hole on the maximum forming force, joint load capacity, and energy consumption of the joining process will be presented in further part of the paper.

The largest change in the outer diameter of the joint (ϕd_2) was obtained for the joint after increasing the rivet hole diameter from 2.0 to 2.5 mm (Fig. 20). The other values of the rivet dimensions in the joint are presented in Fig. 21. It would seem that for a solid rivet and for rivets with a hole diameters smaller than 2.5 mm, its stiffness is higher and a larger vertical rivet recess in the sheet material can be obtained. However, the rivet with the largest hole diameter has the smallest top supporting surface. Hence, the flow resistance of the material was lower and the rivet was deeper pressed in the vertical direction. The value of the forming

force was the lowest (Fig. 12), and the parameters of the interlock decreased (Fig. 22).

As the diameter of the rivet hole increased, the rivet depth increased in the direction of the punch forming movement (Fig. 23). The size of the outer diameter of the rivet (ϕd_1), for the case of the solid rivet and the rivet with a 1 mm hole, was at a similar level (Fig. 23). The largest difference was obtained for the rivet with a hole of 2.5 mm, the diameter ϕd_1 decreased by 5.6%, as in the case of the joint with a solid rivet (Fig. 21). The average size (from five measurements) of the interlock (t_u), for the case of joint forming with a rivet with a 2.5 mm hole was 12.5% smaller than for a solid rivet (Fig. 22), but the maximum forming force was 21.5% lower (Fig. 15).

For the “CL/CR” joints formed with punch and “SKB” die, the smallest value of $t_u = 0.27$ mm, the radial recess of the upper sheet material in the lower sheet, was obtained (Fig. 22). However, the highest value of the thinned embossment of the upper sheet, $t_{n\min} = 0.36$ mm, was also obtained. The size of these parameters significantly affects the load capacity of the joint. The use of an additional rivet with a hardness of 400 HV1 resulted in an increase in $t_{n\min}$ parameter in relation to the joint without a rivet by 18.5%. The forming force increased by 40.5% (Figs. 15, 22). In the case of forming with a rivet with a hole of 1.0 mm, the value of

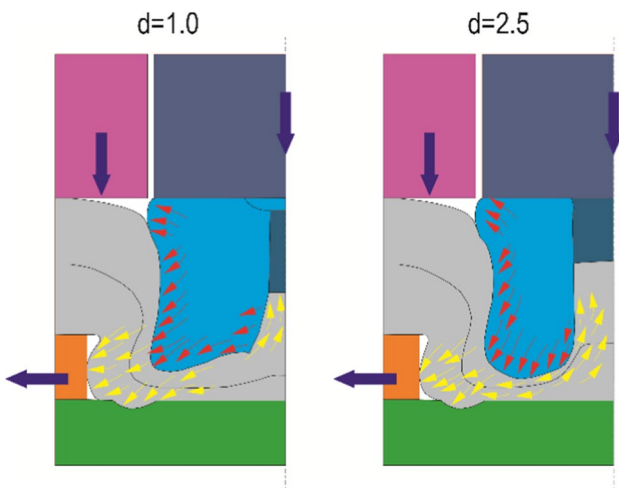


Fig. 19 Mechanism of the rivet and sheet material flow for rivets with 1.0 and 2.5 diameters (d in mm)

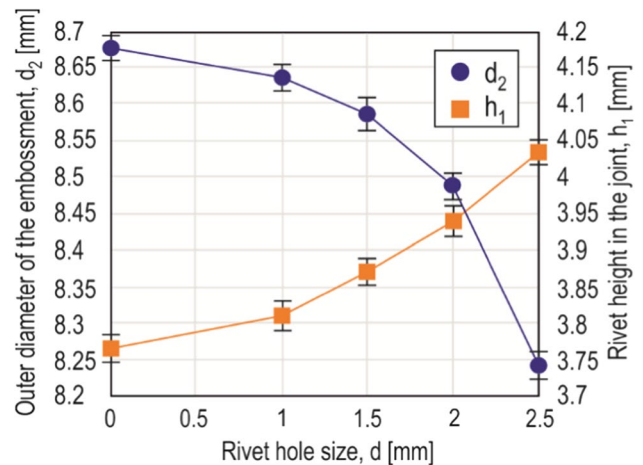


Fig. 20 Rivet hole diameter influence on the ϕd_2 and h_1 “CR/CR” interlock dimensions

Table 5 Comparison of the weight of solid rivet and rivet with through holes

| Parameter | Rivet hole diameters, d , mm | | | | |
|--|--------------------------------|-----------------------|-----------------------|-----------------------|-----------------------|
| | 0 | 1.0 | 1.5 | 2.0 | 2.5 |
| Rivet weight, g_r (kg) | 6.78×10^{-6} | 6.60×10^{-6} | 6.36×10^{-6} | 5.99×10^{-6} | 5.46×10^{-6} |
| Relative rivet weight to a solid rivet, Δ (%) | 100 | 97.35 | 93.81 | 88.35 | 80.53 |
| Rivet weight change, Δg_r (%) | 0 | 2.65 | 6.19 | 11.65 | 19.47 |

$t_{n\ min}$ did not change, but the value of t_u decreased in relation to the solid rivet by 3%. For rivets with holes of 1.5 and 2.0 mm, similar values were obtained as for the rivet with a hole of 1.0 mm. On the other hand, the value of $t_{n\ min}$ parameter increased. Forming the joint with a rivet with a 2.5 mm hole resulted in similar values of the t_u and $t_{n\ min}$ interlock values, and the forming force was 9% higher than for the joint with a solid rivet.

3.3 Joint strength

During the tensile shear test, the gradual loading of the lap joint caused the bending of the sheet from the rivet side (Fig. 24). As the load increased, the deflection of the rivet increased until it was completely pulled out from the bottom sheet. At the same time, the embossment of the upper sheet was damaged, in the narrowing of the interlock cylindrical (Fig. 25). For the joints, with the rivet with a diameter hole of 2.5 mm, the largest rotation of the rivet (Fig. 25e) was obtained during tensile shear tests.

In the case of “CR/CR” tensile shear tests, the failure modes (was pull out with neck fracture) were the same for joints with solid rivet and rivets with through hole (Fig. 26).

The top sheet (from the punch side) was bent (detail “1” in Fig. 26b). The bottom sheet (from the die side) was

not deformed, there was a slight deformation (bent) in the embossment area (detail “2” in Fig. 26b).

For “CL/CR” joints, the failure mode was neck fracture: sheets were separated by shearing in the neck (Fig. 26a). Sheets were not bended, and part of the upper sheet interlock remained in the bottom sheet.

For the joints made with the use of the “SKB” die with an additional rivet (“CR/CR”), the value of the maximum shear force was on average 85% higher than for the joints made without the rivet (“CL/CR”) (Fig. 27). It was also obtained that the maximum shear force for the “CR/CR” joint was for a displacement value of around 1.15 mm, and for the “CL/CR” joint, it was a value of 0.80 mm. It can also be observed, in Fig. 27, that the load curve for the “CR/CR” drops quite sharply after exceeding the maximum value. The load curves were different for the joints without the additional rivet. After achieving the maximum load force (displacement around 0.9 mm) the required force to destroy the joint slowly decreased until displacement around $s = 1.7$ mm. Different mechanisms of joints failure were responsible for this different in load-elongation diagrams shapes. For

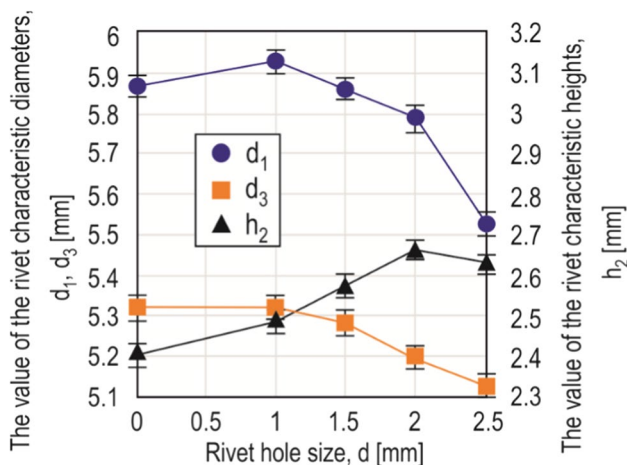


Fig. 21 Rivet hole diameter influence on the ϕd_1 , ϕd_3 and h_2 “CR/CR” interlock dimensions

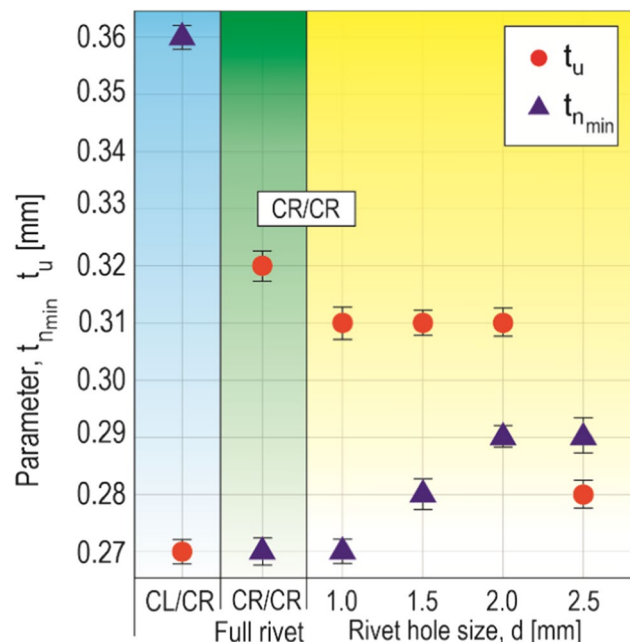


Fig. 22 The $t_{n\ min}$ and t_u interlock dimensions for different tolls arrangements

Fig. 23 Cross-section profiles comparison of joints with rivet with through hole—solid line, and solid rivet dashed line (d in mm)

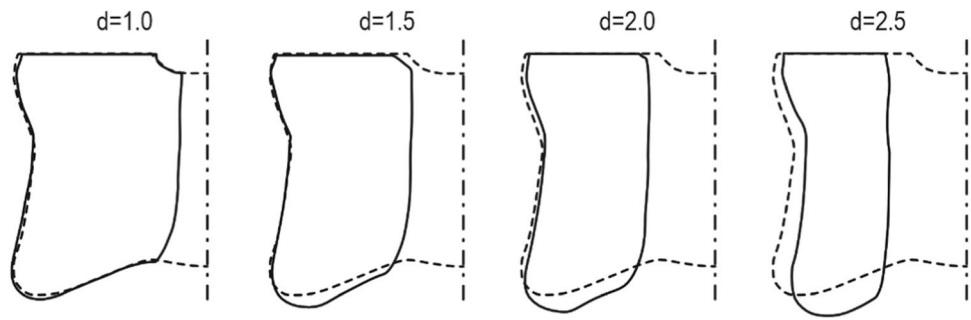


Fig. 24 Example of “CR/CR” joints deformation during tensile shear tests



each tools' arrangement (“CL/CR” and “CR/CR” joints), five samples were tested in tensile shear test. The load-elongations diagrams, for joints with an additional rivet with different hole diameters, were similar in all phases of forming joints (Fig. 28). In Fig. 29, examples of load-elongation diagrams, for each “CR/CR” joints, were presented with load-elongation diagram for “CR/CR” joint with a solid rivet.

4 Dissipated energy

On the basis of the load-elongations diagrams, obtained in the tensile shear test of lap joints, the calculation of specific values of energies was made (Fig. 30). Values were calculated in accordance with the ISO 12996: 2013 standard. The use of an additional rivet increased the total destruction energy of the joint. However, the highest values of the

dissipated energy up to fracture was obtained for the “CR/CR” joints with a 1.5 mm rivet hole diameter. Also, the highest value of dissipated energy up to maximum load force, was obtained for the rivet with a 1.5 mm hole (Fig. 30). The highest values of dissipated energy up to the 0.3 maximum load force was obtained for the “CR/CR” joint formed with a rivet with a hole diameter of 1.0 mm.

In the case of the “CL/CL” and “CR/CR” joints, the displacements up to fracture s_{fract} were at a similar level (Fig. 31). Higher value of displacement was obtained to achieve the maximum load capacity of the joint. The use of an additional rivet with a hole diameter of 1.0, 1.5, 2.0 caused of that the joint maximum load capacity was obtained for a similar displacement $s_{F_{\text{smax}}}$.

Comparing the results obtained for the “CR/CR” joints with those for the “CL/CR” joints, it can be concluded that

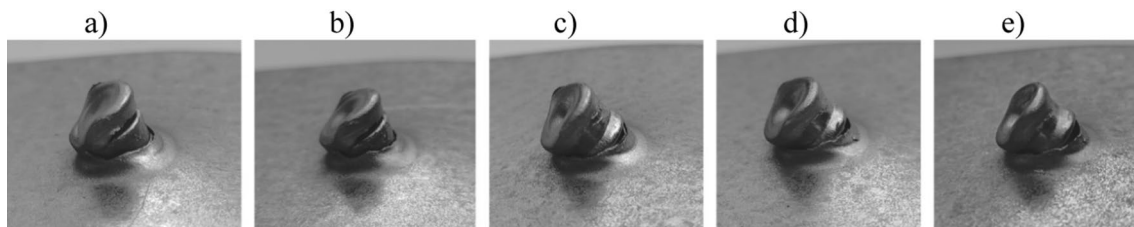


Fig. 25 Influence of the rivet hole diameter on the joint deformation after tensile shear tests: **a** without hole d (solid rivet), **b** 1.0, **c** 1.5, **d** 2.0, **e** 2.5 (d in mm)

Fig. 26 Tested lap joints specimens after tensile shear tests: **a** “CL/CR”, **b** “CR/CR”

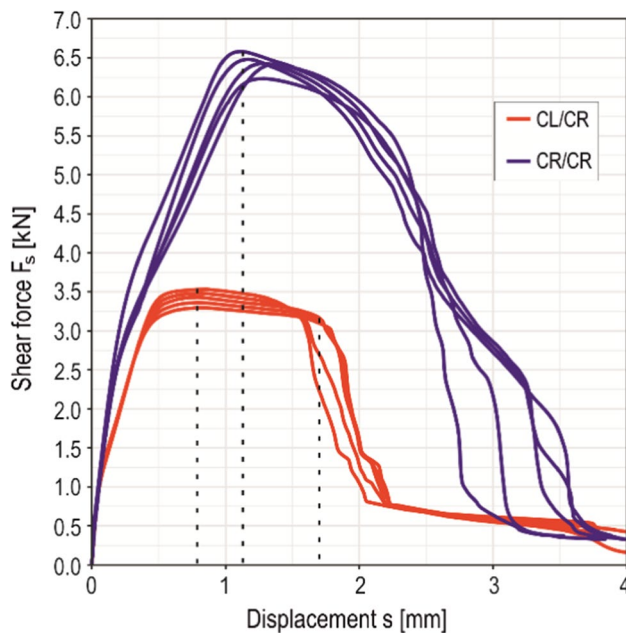
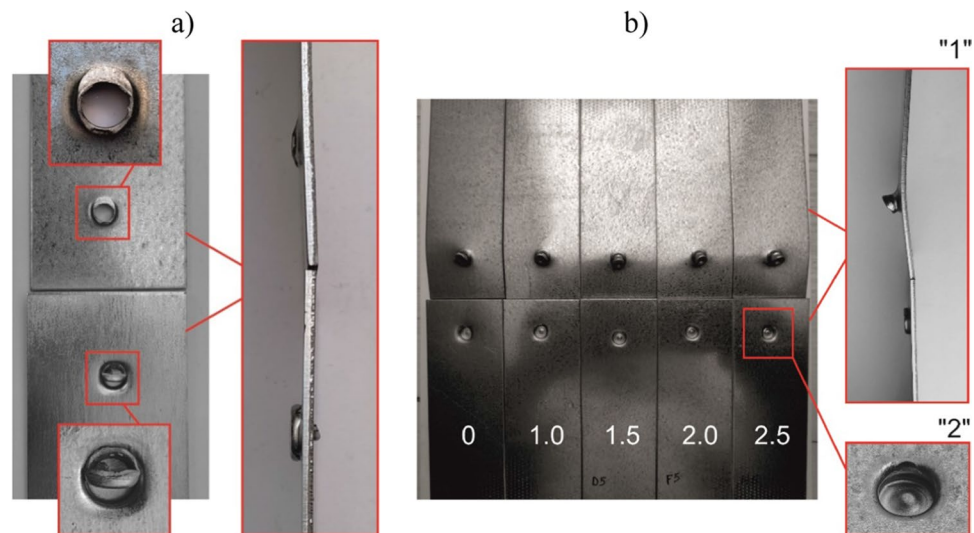


Fig. 27 Load-elongation diagrams from the tensile shear tests of “CL/CR” and “CR/CR” joints

the greatest increase of the forming force was obtained for the case of using a solid rivet (Fig. 32). And the greatest increase in dissipated energy up to maximum load was obtained for the joint with a rivet with a hole diameter of 1.5 mm. In the case of a joint with a solid rivet and with a hole diameter of 1.5 mm, similar values of the increase in joint shear force were obtained, compared to the “CL/CR” joint. Comparing the increases in the maximum load capacity of the joints, it can be concluded that for the rivet with a hole of 1.5 mm, the highest increase in dissipated

energy up to fracture was obtained (by 170%), the increase in the maximum load capacity (by 87%), and unfortunately the increase in the forming force (by 30%) compared to the “CL/CR” joint. The smallest increase in dissipated energy up to maximum load force was obtained for the rivet with a 2.5 mm hole diameter (by 8%), and at the same time, an increase in the maximum load force was obtained (by 80%) compared to the case of the “CL/CR” joint.

5 Conclusions

The experimental tests proved the importance of using an additional rivet for the changing of pressed joint geometric structure and its load capacity. There is no doubt that forming the clinching joints requires the least forming force and forming energy. The modification of the joining process by using an additional solid rivet allows for a very large increase of joint load capacity. But it also causes a large increase of the forming force. The use of an additional rivet, with a through hole, leads to an increase of the joint load capacity and a decrease in the forming force. The most important conclusions from the research are:

- the use of an additional rivet changes the joint failure mechanism: for “CL/CR” (without rivet) the neck fractures were obtained and for “CR/CR” the pull out with neck fractures were obtained;
- the highest value of neck thickness ($t_{n \min} = 0.36$ mm) was obtained for the “CL/CR” joint, and for the interlock size ($t_n = 0.32$ mm) for the joint with a solid rivet (“CR/CR”);
- the use of an additional element (rivet) in joint forming process resulted in an increase of the maximum shear-

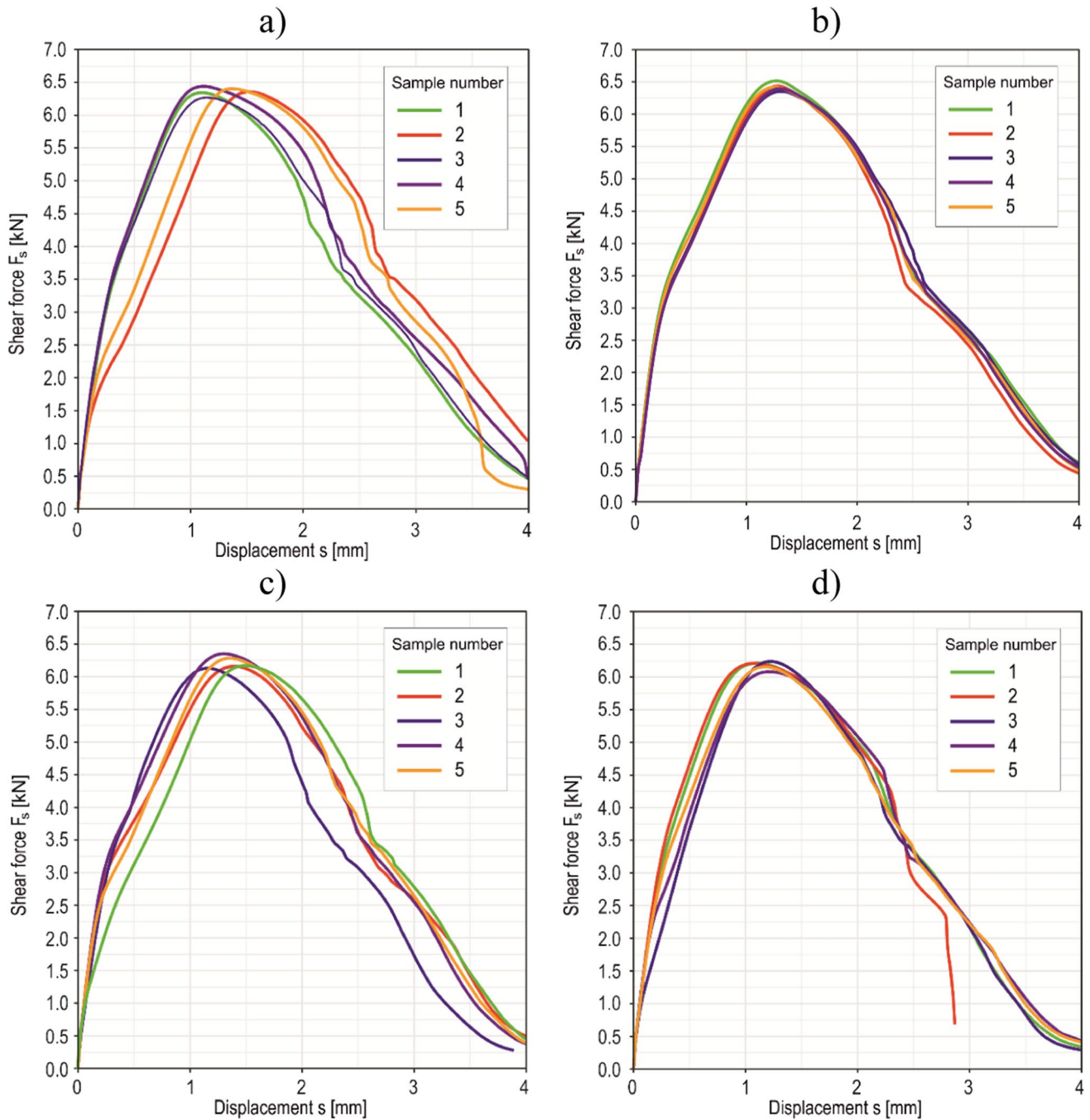


Fig. 28 Load-elongation diagrams from the tensile shear tests of “CR/CR” joints with rivet hole diameters (d): **a** 1.0, **b** 1.5, **c** 2.0, **d** 2.5 (d in mm)

- ing force of the lap joint by 87% (compared to the joint without the rivet);
- the value of the through hole diameter in an additional rivet do not impact significantly on the maximum load force—for all diameters, the joint load capacity was about 80% of the “CR” with solid rivet joint load capacity;
- for the “CR/CR” joint with the rivet with a 2.5 mm hole diameter the maximum load capacity increased about 80% (the dissipated energy up to maximum load force also increased), however, the forming force increased about 8% compared to “CL/CR” joint (without an additional rivet);

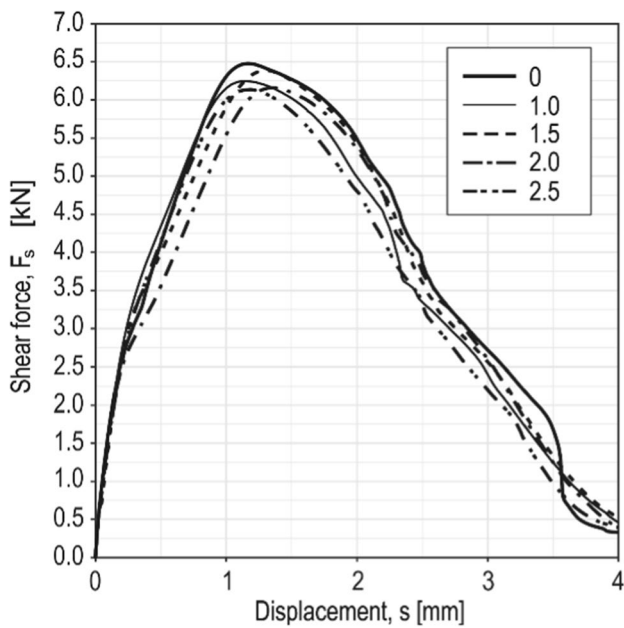


Fig. 29 Examples of load-elongations diagrams from the tensile shear tests of “CR/CR” joints with different hole diameters (d in mm)

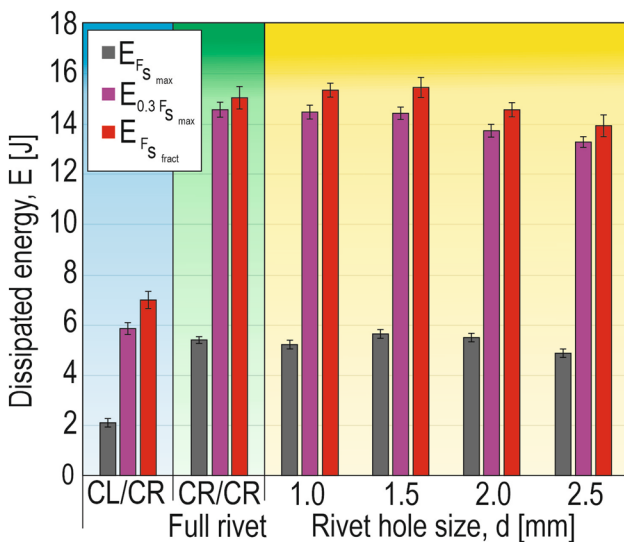


Fig. 30 Dissipated energy averages for “CL/CR” and “CR/CR” joints

- by increasing the through hole diameter in rivet the forming force is significantly decreasing, so the forming energy is lower than for solid rivet;
- the additional rivet in “CR/CR” joints caused that dissipated energy up to maximum load force increased about 158% compared to joint without an additional rivets.

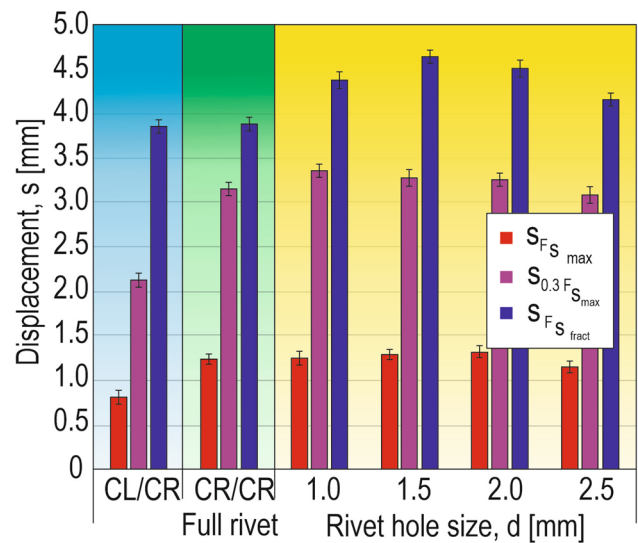


Fig. 31 Displacements average from the tensile shear test (in accordance to ISO 12996-2013 standard)

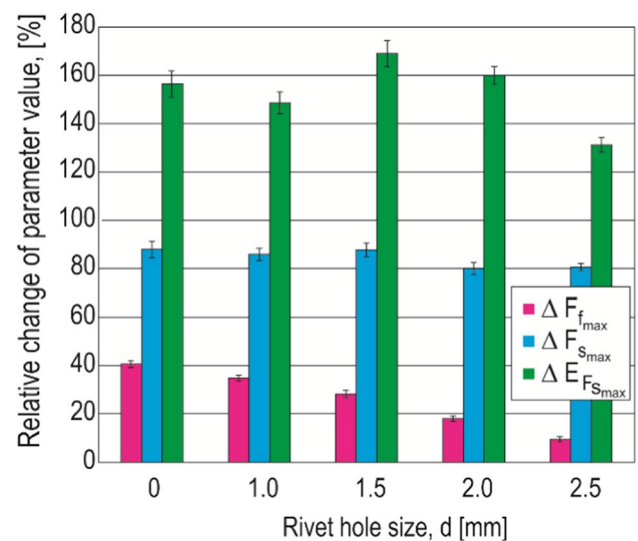


Fig. 32 The relative change of “CR/CR” joint parameters, with different hole diameters, ($F_{f_{max}}$ —forming force, $F_{s_{max}}$ —maximum load, $E_{F_{s_{max}}}$ —dissipated energy up to maximum load force) in relation to the “CL/CR” joints parameters

Declarations

Conflict of interest On behalf of all authors, the corresponding author states that there is no conflict of interest.

Ethical approval This article does not contain any studies with human participants or animals performed by any authors.

Open Access This article is licensed under a Creative Commons Attribution 4.0 International License, which permits use, sharing, adaptation, distribution and reproduction in any medium or format, as long as you give appropriate credit to the original author(s) and the source, provide a link to the Creative Commons licence, and indicate if changes were made. The images or other third party material in this article are included in the article's Creative Commons licence, unless indicated otherwise in a credit line to the material. If material is not included in the article's Creative Commons licence and your intended use is not permitted by statutory regulation or exceeds the permitted use, you will need to obtain permission directly from the copyright holder. To view a copy of this licence, visit <http://creativecommons.org/licenses/by/4.0/>.

References

- Ou H, Tang X, Xiao J, Wang Y, Ma Z. Lightweight body-in-white design driven by optimization technology. *Autom Innov*. 2018;1:255–62. <https://doi.org/10.1007/s42154-018-0032-x>.
- Groche P, Wohletz S, Brenneis M, Pabst C, Resch F. Joining by forming—a review on joint mechanisms, applications and future trends. *J Mater Process Technol*. 2014;214(10):1972–94. <https://doi.org/10.1016/j.jmatprotec.2013.12.022>.
- He X. Clinching for sheet materials. *Sci Technol Adv Mater*. 2017;18(1):381–405. <https://doi.org/10.1080/14686996.2017.1320930>.
- Peng H, Chen C, Zhang H, Ran X. Recent development of improved clinching process. *Int J Adv Manuf Technol*. 2020;110:3169–99. <https://doi.org/10.1007/s00170-020-05978-4>.
- Zhang X, Chen C, Peng H. Recent development of clinching tools and machines. *Int J Adv Manuf Technol*. 2022;121:2867–99. <https://doi.org/10.1007/s00170-022-09428-1>.
- Zhang X, Chen C. Experimental investigation of joining aluminium alloy sheets by stepped mechanical clinching. *J Market Res*. 2022;19:566–77. <https://doi.org/10.1016/j.jmrt.2022.05.046>.
- Eshtayeh MM, Hrairi M. Recent and future development of the application of finite element analysis in clinching process. *Int J Adv Manuf Technol*. 2016;84:2589–608. <https://doi.org/10.1007/s00170-015-7781-z>.
- He X, Zhang Y, Xing B, Gu F, Ball A. Mechanical properties of extensible die clinched joints in titanium sheet materials. *Mater Des*. 2015;71:26–35. <https://doi.org/10.1016/j.matdes.2015.01.005>.
- Mucha J, Witkowski W. The experimental analysis of the double joint type change effect on the joint destruction process in uniaxial shearing test. *Thin Walled Struct*. 2013;66:39–49. <https://doi.org/10.1016/j.tws.2013.01.018>.
- Mucha J, Witkowski W. The clinching joints strength analysis in the aspects of changes in the forming technology and load conditions. *Thin Walled Struct*. 2014;82:55–66. <https://doi.org/10.1016/j.tws.2014.04.001>.
- Chen C, Zhao S, Cui M, Han X, Fan S. Mechanical properties of the two-steps clinched joint with a clinch-rivet. *J Mater Process Technol*. 2016;237:361–70. <https://doi.org/10.1016/j.jmatprotec.2016.06.024>.
- Chen C, Zhao S, Cui M, Han X, Ben N. Numerical and experimental investigations of the reshaped joints with and without a rivet. *Int J Adv Manuf Technol*. 2016;88(5–8):2039–51. <https://doi.org/10.1007/s00170-016-8889-5>.
- Chen C, Zhao S, Han X, Cui M, Fan S. Optimization of a reshaping rivet to reduce the protrusion height and increase the strength of clinched joints. *J Mater Process Technol*. 2016;234:1–9. <https://doi.org/10.1016/j.jmatprotec.2016.03.006>.
- Chen C, Ran X, Pan Q, Zhang H, Yi R, Han X. Research on the mechanical properties of repaired clinched joints with different forces. *Thin Walled Struct*. 2020;152:106752. <https://doi.org/10.1016/j.tws.2020.106752>.
- Chen C, Li Y, Zhang H, Li Y, Pan Q, Han X. Investigation of a renovating process for failure clinched joint to join thin-walled structures. *Thin Walled Struct*. 2020;151:106686. <https://doi.org/10.1016/j.tws.2020.106686>.
- Shi C, Li H, Chen C, Ouyang Y, Qin D. Experimental investigation of the flat clinch–rivet process. *Thin Walled Struct*. 2022;171:108612. <https://doi.org/10.1016/j.tws.2021.108612>.
- Ren X, Chen C, Peng H, Ran X, Qin D. Experimental investigation on the cross-tensile properties of tubular rivet-reinforced joints. *Proc Inst Mech Eng Part E J Process Mech Eng*. 2022;236(2):480–90. <https://doi.org/10.1177/09544089211043629>.
- Chen C, Wu J, Li H. Optimization design of cylindrical rivet in flat bottom riveting. *Thin Walled Struct*. 2021;168:108292. <https://doi.org/10.1016/j.tws.2021.108292>.
- Zhang Y, Wang C, Shan H, Li Y, Luo Z. High-toughness joining of aluminium alloy 5754 and DQSK steel using hybrid clinching–welding process. *J Mater Process Technol*. 2018;259:33–44. <https://doi.org/10.1016/j.jmatprotec.2018.04.021>.
- Sampaio RFV, Pragana JPM, Clara RG, Bragança IMF, Silva CMA, Martins PAF. New self-clinching fasteners for electric conductive connections. *J Manuf Mater Process*. 2022;6(6):159. <https://doi.org/10.3390/jmmp6060159>.
- He Y, Yang L, Zong P, Dang J, Ma J. Rotated clinching process for two-layer metallic sheets. *Int J Adv Manuf Technol*. 2022;119:3819–31. <https://doi.org/10.1007/s00170-021-08474-5>.
- EN 10346:2015 (2015) Continuously hot-dip coated steel flat products for cold forming—technical delivery conditions, European Committee for Standardization
- ISO 6507-1:2018 (2018) Metallic materials—Vickers hardness test—part 1: test method, technical committee ISO/TC 164/SC 3 hardness testing
- ISO 12996:2013 (2013) Mechanical joining—destructive testing of joints—specimen dimensions and test procedure for tensile shear testing of single joints, technical committee ISO/TC 44/SC 6 resistance welding and allied mechanical joining

Publisher's Note Springer Nature remains neutral with regard to jurisdictional claims in published maps and institutional affiliations.